Optical generation of inversion walls in nematic liquid crystals

I. Jánossy[1] and S. K. Prasad[2]
[1]*Research Institute for Solid State Physics and Optics of the Hungarian Academy of Sciences, P. O. Box 49, H-1525 Budapest, Hungary*
[2]*Center for Liquid Crystal Research, P. O. Box 1329, Jalahalli, Bangalore 560013, India*
(Received 2 November 2000; published 27 March 2001)

An approach to generate inversion walls in nematic liquid crystals using optical reorientation is described. Planar cells with small pretilt are exposed to an oblique laser beam, which reverses the director tilt angle within the irradiated area. During the electric Freedericksz transition an inversion wall surrounding the laser spot is formed. A theoretical relation is provided for the critical laser intensity necessary to produce an inversion wall. Experimental results in a dye-doped nematic are in satisfactory agreement with the theory.

DOI: 10.1103/PhysRevE.63.041705 PACS number(s): 61.30.Jf, 42.70.Df

I. INTRODUCTION

The study of various types of defects in liquid crystals (walls, lines, and point singularities) is an important area for both fundamental and applied liquid crystal research. Defects often appear spontaneusly in unoriented samples, but they can also be generated in controlled ways. One technique is to impose boundary conditions which are incompatible with a smooth director configuration within the liquid crystal sample [1–3]. In such situations defects with singular cores are formed. In other experiments, coreless domain walls are created in uniformly aligned liquid crystal cells, by applying external magnetic or electric fields. A classic example of the latter process occurs in a planarly oriented nematic film, subjected to a field perpendicular to the substrates. Above the Freedericksz threshold, the sample breaks up into randomly distributed regions with positive and negative tilt angles of the director. The domains formed in this way are separated by narrow walls in which the tilt angle changes from positive to negative values. Some properties of such walls were described long ago by Leger-Quercy, and more recently by Gilli *et al.* [4].

In this paper, we demostrate the possibility of creating domain walls in nematic liquid crystals with the help of optical reorientation. The procedure is sketched in Fig. 1. A conventional sandwich-type cell is used; the two substrates are coated with polymer layers and rubbed unidirectionally. As is well known, this kind of surface treatment ensures a quasiplanar alignment of nematic materials with a small pretilt. The pretilt prevents the formation of domains during an electric-field induced reorientation. To generate a wall, the cell is illuminated by a laser beam in the absence of electric field. Choosing a proper angle of incidence and polarization of the light beam, the bulk tilt angle can be reversed within the illuminated area with respect to that in the outer region [Fig. 1(a)]. Above a critical laser intensity, the light-induced reorientation becomes sufficient to force the formation of a domain with inverted tilt angle when the electric field is applied. This domain is confined to the illuminated area; hence a wall forming a closed loop around the laser spot appears [Fig. 1(b)].

The aim of the current paper is to discuss the conditions for domain generation. In Sec. II, we show that the critical laser intensity, above which a domain wall forms under the influence of an applied electric field, is a fraction of the optical Freedericksz threshold; the ratio between the two thresholds is of the order of magnitude of the pretilt. The critical intensity can be further reduced drastically if dye dopants are added to the nematic material. We experimentally demonstrate the formation of loops in a dye-doped cell illuminated with a He-Ne laser of few mW. In the experiments we also check quantitatively the theoretical predictions for domain formation. However, we postpone, the detailed description of the static and dynamic properties of the wall to a future publication.

II. THEORETICAL CONSIDERATIONS

Optical reorientation in nematic liquid crystals was studied extensively in the past decades. For a review containing the latest results; see Ref. [5].

In order to discuss the conditions of domain formation

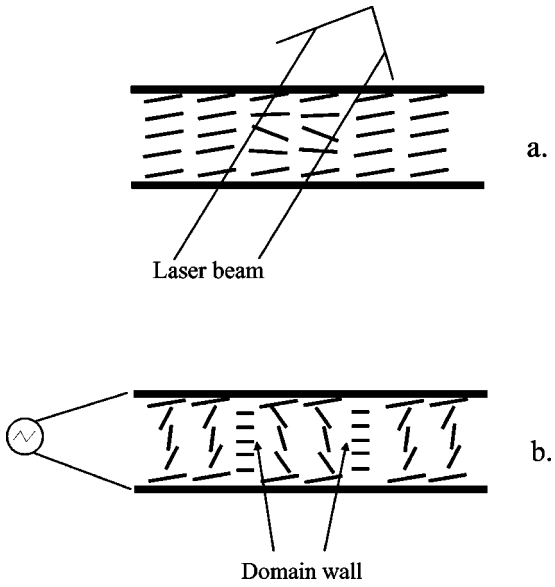

FIG. 1. Schematic representation of the generation of the inversion wall. Director configuration in the presence of a laser beam without electric field (a) and in the presence of a strong electric field (b).

quantitatively, we calculate the director distribution under the influence of simultaneously applied electric and optical fields. Such calculations were published a long time ago in the literature [6–8]; here we apply the general formalism to our special problem. First an infinite planar wave is considered. The plane of incidence and the light polarization is in the xz plane, where the z axis is along the sample normal, and the x axis is parallel to the rubbing direction. The static field is applied along z. In this case the director is a function only of the z coordinate, and can be characterized by the tilt angle θ with respect to the x axis. We define the direction of the x axis in a way that the pretilt should be positive; a positive angle of incidence of the light beam means that the x component of the wave vector is positive.

For transparent nematics the balance of torque reads

$$K\frac{d^2\theta}{dz^2}+\epsilon_0\Delta\epsilon_{st}E_{st}^2\frac{\sin 2\theta}{2}+\epsilon_0(\Delta\epsilon_{opt})E_{opt}^2\frac{\sin 2\Psi}{2}=0. \tag{2.1}$$

The first term represents the elastic torque in the one-constant approximation, and K is the Frank elastic constant. The second and third terms correspond to the static electrical and optical torque. E and $\Delta\epsilon$ denote the effective electric field strength and the dielectric anisotropy for the static and optical fields, respectively, as indicated by the subscripts st and opt. Ψ is the angle between the polarization direction of the light beam and the director. $\Delta\epsilon_{opt}=n_e^2-n_o^2$, where n_e is the extraordinary and n_o is ordinary refractive index. The boundary conditions are

$$\theta(-L/2)=\theta(L/2)=\theta_p, \tag{2.2}$$

where θ_p is the pretilt, L is the sample thickness, and $z=0$ is at the midplane of the cell.

In order to simplify mathematics, we neglect the variations of the applied static field along the z direction, i.e., we assume $E_{st}=V/L$, where V is the applied voltage. Furthermore, we express the optical torque Γ^{opt} with the help of the external angle of incidence (β) and the intensity of the incoming light (I). As shown in the Appendix, in the geometrical optics approximation

$$\Gamma^{opt}=-\frac{\Delta\epsilon_{opt}I}{cn_o^2}[f_1(\theta)\sin^2\beta+f_2(\theta)\cos^2\beta + f_3(\theta)\sin 2\beta/2] \quad (c \text{ is the velocity of light}) \tag{2.3}$$

where

$$f_1(\theta)=\frac{\sin 2\theta}{2n_o^2\gamma}, \quad f_2(\theta)=-n_e^2\frac{\sin 2\theta}{2\gamma},$$

$$f_3(\theta)=\frac{n_o^2\cos^2\theta-n_e^2\sin^2\theta}{n_o^2\gamma} \quad \text{with} \quad \gamma=\left(1+\frac{\Delta\epsilon_{opt}}{n_o^2}\sin^2\theta\right)^2.$$

Introducing a normalized z coordinate $Z=z/L$, a reduced voltage $U=V/V_{Fr}$, where $V_{Fr}=\pi\sqrt{K/\epsilon_0\Delta\epsilon_{st}}$ is the Freedericksz threshold voltage, and a reduced intensity $F=I/I_0$ with $I_0=\pi^2/L^2(Kcn_o^2/\Delta\epsilon_{opt})$, Eq. (2.1) becomes

$$\frac{d^2\theta}{dZ^2}=-\pi^2\{U^2\sin 2\theta/2-F[f_1(\theta)\sin^2\beta+f_2(\theta)\cos^2\beta + f_3(\theta)\sin\beta\cos\beta]\} \quad \text{with} \quad \theta(-1/2)=\theta(1/2)=\theta_p. \tag{2.4}$$

Some solutions of the above equation are presented in Fig. 2. The curves show the director tilt angle at the midplane of the cell ($z=0$) as a function of the applied voltage, at fixed pretilt, and at different laser intensities. Only stable solutions are plotted. Below the electric Freedericksz threshold there is only one solution, while above the threshold there are two of them: one approaching $+\pi/2$ at high voltages, the other one $-\pi/2$. In the absence of the light beam, the positive branch extends to zero voltage, while the negative branch becomes unstable near the Freedericksz threshold [Fig. 2(a)]. For sufficiently strong light intensities, the situation is reversed [Fig. 2(b)]. The transition from the first case to the second occurs at a critical intensity I_{cr}, where the two branches join at a voltage slightly below the Freedericksz threshold [Fig. 2(c)].

In experiments the static electric field is increased from zero to a value well above the Freedericksz threshold, at fixed laser intensity. For zero voltage there is only one stable director configuration, which corresponds to the positive branch if $I<I_{cr}$, and to the negative branch if $I>I_{cr}$. Assuming that during the increase of the voltage no transition from one branch to the other can occur, we expect that the steady state tilt angle at high voltages will converge to $+\pi/2$ or to $-\pi/2$, depending whether I is lower or higher than I_{cr}.

It should be emphasized that the optical field plays a role only in the initial part of the process. Once the director field stabilizes at negative tilt angles (at $I>I_{cr}$), it remains there even if the laser beam is switched off. When the optical field is removed, the maximum tilt angle will be shifted to the *negative* branch of the $F=0$ curve [Fig. 2(a)]. A transition to the positive branch will occur only when the voltage is decreased below the critical U value, at which the negative branch for $F=0$ becomes unstable.

An analytical expression for the critical intensity can be derived in the following way. For small pretilts and deformations, Eq. (2.3) can be linearized with respect to θ. In this limit $f_1\approx\theta/n_o^2$, $f_2\approx-n_e^2\theta$, and $f_3\approx 1$. Equation (2.3) becomes

$$\frac{d^2\theta}{dZ^2}=-\pi^2[\tilde{U}^2\theta-F\ \sin 2\beta/2], \tag{2.5}$$

with

$$\tilde{U}^2=U^2+[\sin^2\beta/n_o^2-n_e^2\cos^2\beta]F.$$

The solution of Eq. (2.5) is

$$\theta = \theta_0 \cos \pi \tilde{U} Z + \frac{F}{\tilde{U}^2} \frac{\sin 2\beta}{2} \quad \text{with}$$

$$\theta_0 = \left(\theta_p - \frac{F}{\tilde{U}^2} \frac{\sin 2\beta}{2} \right) \Big/ \cos \frac{\pi}{2} \tilde{U}. \tag{2.6}$$

For $\tilde{U} \to 1$, θ_0 diverges to infinity. The divergence goes toward positive values if $\theta_p > F \sin 2\beta/2$, and to negative ones if $\theta_p < F \sin 2\beta/2$. At the critical intensity the two terms are equal, i.e., $F_{cr} = 2\theta_p / \sin 2\beta$.[1] Using the definition of F, we obtain

$$I_{cr} = \frac{2\theta_p}{\sin 2\beta} I_0 = \frac{2\theta_p}{\sin 2\beta} \frac{\pi^2 n_o^2 c K}{L^2 \Delta \epsilon_{opt}}. \tag{2.7}$$

The above relation can be easily extended to the case with unequal splay and bend elastic contants; for small pretilts K has to be replaced with the splay elastic constant K_1.

It is interesting to compare the critical intensity I_{cr} with the threshold intensity for the optical Freedericksz transition, which for a homeotropic cell is [9]

$$I_{Fr} = \frac{\pi^2 n_e^2 c K}{L^2 n_o \Delta \epsilon_{opt}}. \tag{2.8}$$

Comparing Eqs. (2.7) and (2.8), one finds $I_{cr}/I_{Fr} = 2\theta_p n_o^3 / (n_e^2 \sin 2\beta)$. With $\beta = 45°$, $n_e = 1.75$, $n_o = 1.52$, and $\theta_p = 2°$, obtain $I_{cr} \approx 0.09 I_{Fr}$, i.e., the critical light intensity necessary to reverse the director tilt angle in an electric-field induced deformation is a fraction of the Freedericksz threshold intensity.

As a next step, we consider a broad, but finite, beam with a smooth radial intensity distribution. In particular, we assume that the light intensity changes only slightly at distances comparable to the sample thickness. In this limit, one can neglect transverse effects arising from variations of the director field along the radial direction, and assume that the electric-field-induced director reorientation is sensitive to the local value of the input intensity only. Whenever the light intensity at the beam axis exceeds the critical value, upon applying the field a region with reversed tilt angle will be formed around the center of the beam, while for the beam the tilt angle remains positive. The two regions are separated by a wall, extending along the loop, where the condition $I = I_{cr}$ is fulfilled.

As an example, we consider a Gaussian beam with an intensity distribution $I = P/\pi w_0^2 \exp\{-w^2/w_0^2\}$ where P is the power and w is the distance from the optical axis of the beam. The local input intensity at a point with transverse coordinates x and y is

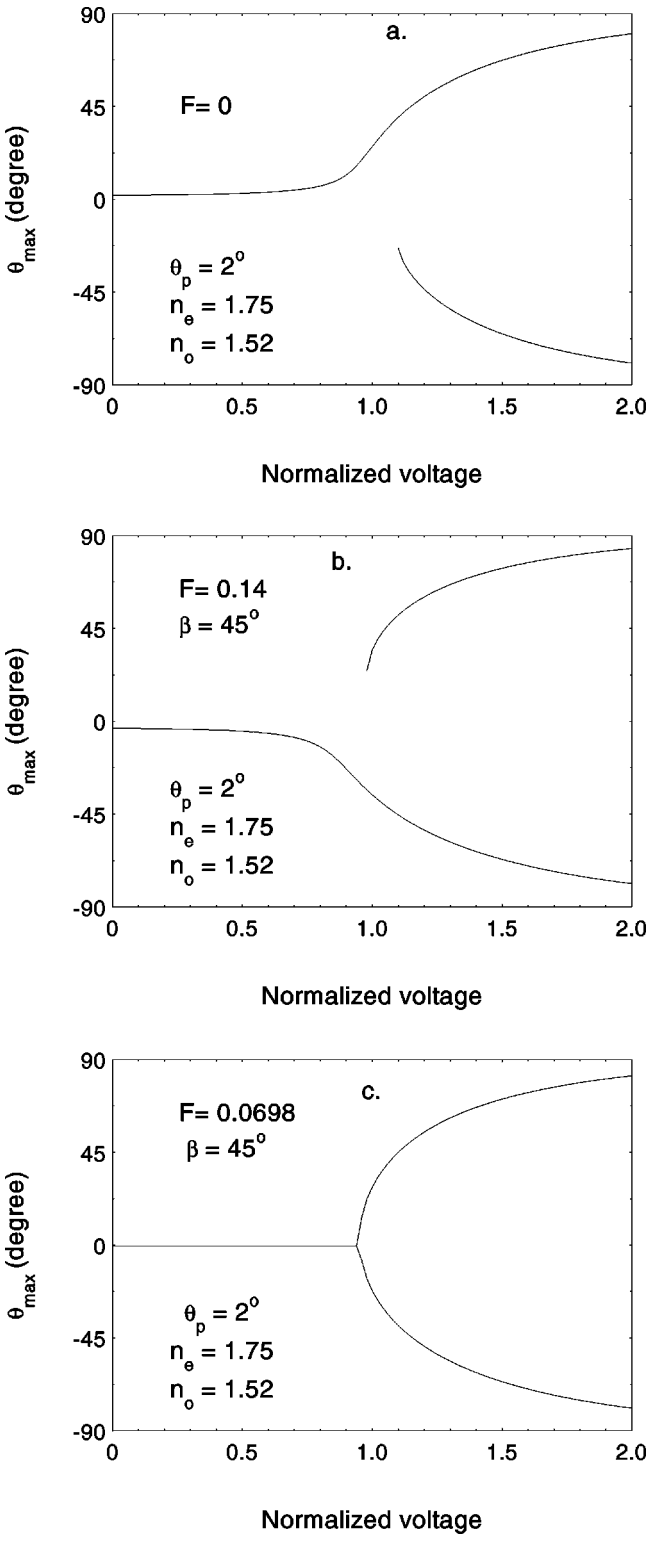

FIG. 2. The maximum tilt angle as a function of the applied voltage for different laser intensities. $F = 0$ (a), $F = 0.14$ (b), and $F = 0.0698$ (c).

[1]Although the above argument might not be completely satisfactory from the point of view of pure mathematics, results from numerical calculation are in agreement with the proposed relation.

$$I(x,y)=\frac{P}{\pi w_0^2}\exp\{-x^2\cos^2\beta/w_0^2-y^2/w_0^2\} \qquad (2.9)$$

where the $x,y=0$ point coincides with the beam axis. The condition $I(x,y)=I_{cr}$ is satisfied along an ellipse, obeying the equation

$$\frac{x^2}{R^2/\cos^2\beta}+\frac{y^2}{R^2}=1 \quad \text{with} \quad R=w_0\sqrt{\ln\frac{P}{\pi w_0^2 I_{cr}}}. \qquad (2.10)$$

R is the charcteristic initial linear dimension of the loop, equal to the half length of its short axis.

Transverse variations of the director field, neglected above, lead to the shrinkage and disappearance of the loop [4]. Our approach is valid only if this process is slow compared to the formation of the domain wall. From a simple dimensional analysis, one expects that the characteristic time for wall formation is of the order of $\gamma L^2(V_{Fr}/V)^2/K$, where γ is the rotational viscosity, and V is the applied voltage. The initial rate of decrease of the loop size is expected to be of the order of $K/(\gamma R)$ (see Ref. [2]). Combining these two estimates, one finds that if the condition $R \gg L(V/V_{Fr})$ is fullfilled, the loop formation occurs much faster than the shrinkage of the loop; therefore, the two processes are well separated. As shown in Sec. III, this requirement can be readily realized in experiments. It should be noted, however, that when R is comparable or smaller than the sample thickness, transverse effects cannot be disregarded any more in the electric-field-induced reorientation process, and the distinction between wall formation and shrinkage becomes arbitrary.

Finally, we discuss the effect of dye doping. As is well known, the presence of absorbing dyes in nematics can enhance the optical torque considerably [10]. In order to account for the influence of the dyes on the optical reorientation process, a factor ξ has to be added to $\Delta\epsilon_{opt}$ in the expression for Γ_{opt}. ξ depends on the chemical structure of the dye, and is proportional to its concentration [11]. A further effect of the presence of absorbing dyes is the attenuation of the light beam within the nematic layer. It was shown for the optical Freedericksz transition [12] that for not too high absorbances ($A \leqslant 2$) attenuation can be taken into account by averaging the light intensity with respect to the z coordinate. Our numerical calculations, in which we considered attenuation (as described in the Appendix) showed that the same holds for the critical intensity in the present case also. With these two modifications Eq. (2.7) can be generalized for dye-doped systems as

$$I_{cr}^d=\frac{2\theta_p}{\sin 2\beta}\frac{\pi^2 K c n_o^2}{L^2(\xi+\Delta\epsilon_{opt})}\frac{A}{1-e^{-A}}$$
$$=I_{cr}^t\left[(1+\eta)\frac{1-e^{-A}}{A}\right]^{-1}, \qquad (2.11)$$

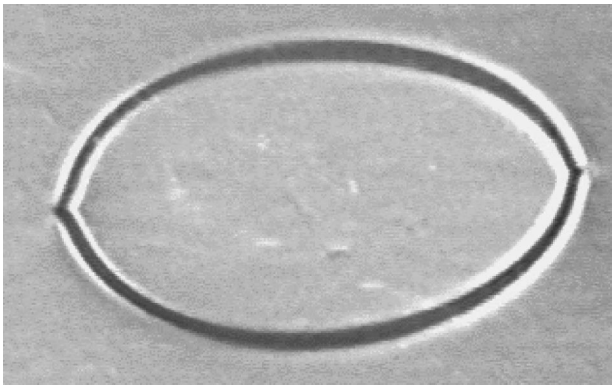

FIG. 3. Photograph of a loop taken in a polarizing microscope.

where the superscripts d and t refer to dye-doped and transparent samples, respectively, and the parameter $\eta=\xi/\Delta\epsilon_{opt}$ gives the ratio between the dye-induced and dielectric parts of the optical torque.

We note that Eq. (2.7), derived for transparent materials, is only meaningful if $0<\beta<\pi/2$, i.e., if the angle of incidence is positive; for negative angle of incidences no loop formation is expected to occur. In dye-doped nematics, however, ξ has often a large negative value [11]. In such cases, the situation is reversed; loop formation is possible only at negative angle of incidences.

III. QUALITATIVE OBSERVATIONS

In most of the experiments commercial cells, supplied by EHC Co., Ltd. (Japan), were used, with thickness of 25 μm. The nematic material was the eutectic mixture E63 from BDH, doped with the dye 1,8 dihydroxy 4,5 diamino 2,7 diisobutyl anthraquinone (AQ1). This dye yields a strong positive enhancment of the optical torque ($\xi>0$) [13]. The optical reorientation was induced by a polarized He-Ne laser beam. The formation of the domain wall was observed either directly in a polarizing microscope, or indirectly, by detecting the far-field laser diffraction pattern.

In Fig. 3, a photograph of a loop is shown. The domain wall formed simultaneuously with the field-induced reorientation of the director, i.e., on the time scale of a second. It was checked that the loop appeared only at extraordinary polarizations and at a positive angle of incidence of the laser beam. These observations provide a strong support that the formation of the domain wall was indeed initiated by optical reorientation.

The initial contour of the loop corresponded to the elliptical intensity distribution of the laser beam, then it rapidly assumed a shape independent from that of the optical field. The eccentricity of this shape depended on the applied voltage; for higher voltages it became more circular. Very characteristic singularities were observed at the ends of the long axis of the loop (Fig. 3). On a longer time scale the loop shrunk, and finally disappeared completely.

The process of formation, transformation, and shrinkage of the domain wall could also be followed also by the observation of the diffraction of the laser beam. A weak self-focusing effect occurred even at zero applied voltage, indi-

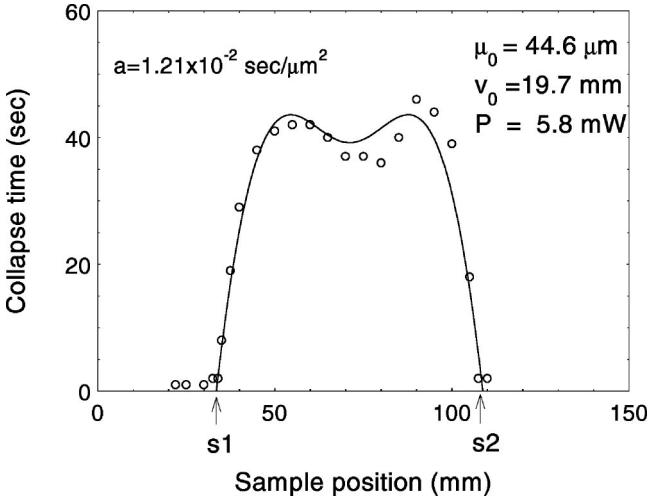

FIG. 4. Collapse time as a function of the sample position.

cating the presence of optical reorientation. When the voltage was switched on, an aberrational ring system developed. Below the threshold for wall formation, the strong diffraction lasted only for a short time ($\approx$a second). When a loop was formed, a new diffraction pattern appeared. The details of this pattern were quite complicated, but essentially it was composed of two different ring systems. In one system, the rings were closely spaced, and the spacing was insensitive to the value of the applied voltage. The rings showed a rapid expansion before the collapse of the loop. The other system consisted of more widely spaced rings; the spacing could be regulated through the applied voltage (with increasing voltage it increased). After the collapse of the loop, no significant self-focusing could be detected.

The observed diffraction pattern might be qualitatively interpreted by assuming that the first ring system originates from the whole loop; the spacing between the rings corresponds to the linear dimension of the loop. The insensitivity of the loop dimension to the magnitude of the applied voltage is in accordance with visual observations. The second ring system can be regarded as a diffraction from the wall itself, with the ring spacing corresponding to the wall thickness. As the wall thickness is inversely proportional to the applied field [4], the diffraction angle should increase when the voltage is increased.

IV. MEASUREMENT OF THE CRITICAL INTENSITY

According to Eq. (2.10), the critical intensity can be determined from a measurement of the loop radius, generated by a beam with known power and spot radius. We found, however, that the investigation of the transient behavior of the diffraction pattern can yield more accurate results. In the experiments, a He-Ne laser beam was focused with a lens, and the sample was translated along the beam axis (the s direction). The angle of incidence was kept at 60°. In the measurements, the time from turning on the applied voltage until the disappearance of laser diffraction (collapse time) was registered at different sample positions.

Experimental data are presented in Fig. 4. As can be seen from the figure, at large distances from the focal point the collapse time corresponded to the transient time of the electric-field-induced reorientation (1-2 sec). On approaching the focal point, at a position $s=s_1$, the collapse time began to increase sharply. In the interval s_1,s_2 around the focal point, it was found to be much longer than the transient time, while for positions $s>s_2$ it again became of the order of a second.

These observations can be interpreted as follows. Within the s_1,s_2 interval, the intensity at the center of the beam exceeds the critical intensity, and a domain wall is formed. In this case, the collapse time corresponds to the time of shrinkage and disappearance of the loop, which is—as discussed in Sec. II, and also confirmed by visual observations—much longer than the director reorientation time in the electric field. The sharp drop in the vicinity of the positions s_1 and s_2 indicates an associated drop of the initial loop size. It seems reasonable to assume that at s_1 and s_2, where the collapse time becomes equal to the transient time, the loop size becomes zero, i.e., at these positions the intensty at the center of the beam is equal to the critical intensity.

To make the above argument quantitative, we consider Gaussian beam propagation. The laser intensity distribution at a distance S from the focus is

$$I=\frac{P}{\pi w_0^2}\exp\{-w^2/w_0^2\} \quad \text{with} \quad w_0=\mu_0(1+S^2/S_0^2)^{1/2}, \tag{4.1}$$

where μ_0 is the spot radius at the focal point and $S_0=2\pi\mu_0^2/\lambda$ is the diffraction length. Combining Eqs. (2.10) and (4.1), for the initial loop dimension one obtains

$$R^2=\mu_0^2(1+S^2/S_0^2)\ln\frac{1+S_{cr}^2/S_0^2}{1+S^2/S_0^2}, \tag{4.2}$$

where the critical distance S_{cr} is related to the critical intensity as

$$I_{cr}=\frac{P}{\pi\mu_0^2(1+S_{cr}^2/S_0^2)}. \tag{4.3}$$

According to Eq. (4.2) the loop size becomes zero at the critical distance S_{cr} from the focal point. As discussed earlier, this occurs at the positions s_1 and s_2; hence $S_{cr}=(s_2-s_1)/2$.

In the present case, we found $S_{cr}=37.6$ mm (see Fig. 4). In order to determine the parameters μ_0 and S_0, the spot radius of the laser beam was measured as a function of s. A good agreement with Eq. (4.1) was obtained with $\mu_0=44.6$ μm and $S_0=19.7$ mm. The laser power was 5.8 mW, which was corrected for absorption losses at the conducting layer of the entrance plate. This was obtained by measuring the transmission loss in a similar cell, filled with a transparent nematic; it was found to be $\approx 6\%$. With these data, from Eq. (4.3) we obtain for the critical intensity $I_{cr}=188$ mW/mm^2.

In order to compare the experimental value of I_{cr} with the theoretical prediction [Eq. (2.11)], the material parameters, the pretilt, and the absorbance due to the presence of the dye have to be known. The material parameters of E63 are taken from Ref. [11]: $K_1 = 0.9 \times 10^{-6}$ dyn, $n_o = 1.52$, and $n_e = 1.74$.

To determine the pretilt, the phase retardation of a weak He-Ne laser beam was measured as a function of the applied voltage. The data below the Freedericksz threshold are sensitive, first of all, to the value of the pretilt. From the analysis of the data $\theta_p = 2.3°$ was obtained [14]. The absorbance was deduced from transmission measurements. Comparing the transmission in a transparent cell and in the dye-doped cell used in the experiment, we found for $\beta = 60°$ and $A = 0.67$.

From the above data we first calculate the theoretical value for the critical intensity in a transparent material. Inserting the numbers into Eq. (2.7), one obtains $I_{cr}^{t} = 120 \times 10^2$ mW/mm^2. As a second step, from the ratio I_{cr}/I_{cr}^{tr} one can evaluate the η parameter; with the help of Eq. (2.11), $\eta = 87$ is found. Although there is no direct independent measurement for this particular dye, the value of η obtained here is in reasonable agreement with data on a very similar anthraquinone dye (AD1 in Ref. [11]).

Returning to the data in Fig. 4, we note that only the s_1 and s_2 values were taken into consideration for the evaluation of I_{cr}. To interpret the data within the $[s_1, s_2]$ region, an assumption has to be made about the connection between the initial loop size and the collapse time. We intend to discuss the kinetic behavior of the loop in more detail in a forthcoming paper. Here we make use only of a relation established empirically during the direct observations of the loop: it was found that the area surrounded by the loop decreased linearly with time. (We note that this result is also in accordance with the assumption made in Sec. II in connection of the rate of decrease of the loop size.) With this conjecture, one obtains

$$t_{col} = aR^2 = aw_0^2 \ln \frac{P}{\pi w_0^2 I_{cr}}. \tag{4.4}$$

The solid line in Fig. 4 corresponds to Eq. (4.4), with the only new fit parameter $a = 1.21 \times 10^{-2}$ sec/μm^2.

The satisfactory agreement between the theoretical curve and the measured data confirms the validity of the proposed mechanism of the laser-induced formation of domain walls. In particular, the theory accounts for the observation that the longest collapse time (largest initial loop size) is obtained at a certain distance from the focal point. We note that the existence of a dip at the focal point follows from the properties of Gaussian beam propagation. The fact that it has been observed experimentally through the observation of the collapse time supports our assumption about the local character of the director response to the optical field.

V. CONCLUSIONS AND OUTLOOK

The method of preparation of domain walls described in the present paper, can have some advantages over the traditional process based on purely electric or magnetic reorientation. While in an electric-field-induced Freedericksz transition domains form spontaneously, here the location, size, and initial shape of a domain can be controlled through the parameters of the incident light beam. It can be even possible to create simultaneuously two or more loops and study their interaction.

We demonstrated that inversion loops can be created with the help of low-power lasers if dye-doped samples are used. The critical intensity can be decreased further with respect to the value reported in our experiment if cells with smaller pretilt are used. It is known that the magnitude of the pretilt can be influenced, e.g., through the rubbing strength [16]. In addition, one of the plates may be prepared with zero pretilt; in this case the critical intensity will be reduced with a factor of 2, compared to a symmetric cell.

On the other hand, it could also be interesting to perform experiments with higher laser intensities, where the optical torque becomes comparable with the static electric torque even above the Freedericksz threshold. Predictions of the behavior of inversion walls under such circumstances were given recently by Srivatsa and Ranganath [15].

Besides the possibility of studying the nature of defects, the method outlined in this paper provides a method for a determination of the strength of the dye-induced optical torque (see Sec. IV). In standard measurements, the η or ξ parameter is deduced from the nonlinear refractive index change [11]. Such measurements have to be corrected, however, for the contribution of thermal effects due to laser heating. In many cases, the thermal nonlinearity is comparable, or even higher than the orientational effect. On the other hand, laser heating affects the critical intensity for wall generation only through the temperature dependence of the material constants, which is usually weak, except near the clearing point.

ACKNOWLEDGMENTS

The work was supported in part by the Copernicus Grant IC15-CT98-0806, and by the Hungarian National Science Research Fund OTKA T-024098. We thank the Indo-Hungarian Academic Exchange Program for supporting the collaboration.

APPENDIX: CALCULATION OF THE OPTICAL TORQUE

The time average of the optical torque excerted by an electromagnetic field on an anisotropic medium is

$$\vec{\Gamma}^{opt} = \vec{D} \times \vec{E}, \tag{A1}$$

where $\vec{D}$ and $\vec{E}$ are the effective amplitudes of the displacement and the electric field vectors, respectively. $\vec{D}$ and $\vec{E}$ are connected through the linear relation

$$\vec{D} = \epsilon_0 \epsilon \vec{E} \quad \text{or} \quad \vec{E} = \frac{1}{\epsilon_0} \epsilon^{-1} \vec{D}. \tag{A2}$$

In uniaxial media $\epsilon_{ij}=\epsilon_\perp\delta_{ij}+\Delta\epsilon n_i n_j$ and $\epsilon_{ij}^{-1}=1/\epsilon_\perp\delta_{ij}-\Delta\epsilon/\epsilon_\perp\epsilon_\parallel n_i n_j$ where $\vec{n}$ is a unit vector along the optical axis, i.e., the director. For optical frequencies, $\epsilon_\perp=n_o^2$, $\epsilon_\parallel=n_e^2$, and $\Delta\epsilon=n_e^2-n_o^2$.

In the case investigated in this paper, $\vec{D}$, $\vec{E}$, and $\vec{n}$ are in the plane of incidence of the light beam (x,y plane). The torque has only a y component:

$$\Gamma^{opt}=D_zE_x-D_xE_z. \tag{A3}$$

With the help of Eq. (A2), D_x and E_z can be expressed through D_z and E_x:

$$D_x=(\epsilon_\parallel E_x+\Delta\epsilon_{opt}/\epsilon_\perp\sin\theta\cos\theta D_z)/(1+\Delta\epsilon/\epsilon_\perp\sin^2\theta),$$

$$E_z=(D_z-\Delta\epsilon\sin\theta\cos\theta E_x)/\epsilon_\perp(1+\Delta\epsilon/\epsilon_\perp\sin^2\theta);$$

thus Eq. (A3) can be rewritten as

$$\Gamma^{opt}=\frac{\Delta\epsilon/\epsilon_\perp}{(1+\Delta\epsilon/\epsilon_\perp)^2}[\sin\theta\cos\theta D_z^2-\epsilon_\perp\epsilon_\parallel\sin\theta\cos\theta E_x^2 +(\epsilon_\perp\cos^2\theta-\epsilon_\parallel\sin^2\theta)D_zE_x]. \tag{A4}$$

In the geometrical optics approximation, the energy transfer from the forward propagating beam to the backward propagating one is neglected. In this limit, in transparent media, D_z and E_x are constant along the beam path. In order to relate these quantities to the input intensity and angle of incidence, we note that outside the sample

$$D_z^2=\frac{I_0}{c}\sin^2\beta,\quad E_x^2=\frac{I_0}{c}\cos^2\beta,\quad D_zE_x=\frac{I_0}{c}\sin\beta\cos\beta. \tag{A5}$$

where I_0 is the intensity of the input beam.

If reflection and absorption losses at the air-substrate and substrate-liquid crystal interfaces are negligible, the same relations hold within the sample. To account for these losses, one can replace I_0 with $I=T_sI_0$, where T_s is the transmission coefficient of the substrate at the entrance face of the sample. With this correction, the combination of Eqs. (A4) and (A5) leads to

$$\Gamma^{opt}=-\frac{\Delta\epsilon I}{c\epsilon_\perp}[f_1(\theta)\sin^2\beta+f_2(\theta)\cos^2\beta+f_3(\theta)\sin 2\beta/2], \tag{A6}$$

where the f functions are

$$f_1(\theta)=\frac{\sin 2\theta}{2\epsilon_\perp\gamma},\quad f_2(\theta)=-\epsilon_\parallel\frac{\sin 2\theta}{2\gamma},$$

$$f_3(\theta)=\frac{\epsilon_\perp\cos^2\theta-\epsilon_\parallel\sin^2\theta}{\epsilon_\perp\gamma}\quad\text{with}\quad\gamma=\left(1+\frac{\Delta\epsilon}{\epsilon_\perp}\sin^2\theta\right)^2.$$

Replacing the ϵ's with the appropriate optical quantities, one arrives at Eq. (2.3).

For weakly absorbing liquid crystals Eq. (2.3) can be generalized by taking into account the gradual decrease of the intensity within the layer. The z dependent intensity can be expressed as

$$I(z)=T_sI_0\exp\left(-\int_{L/2}^{z}\alpha_z dz\right). \tag{A7}$$

α_z can be calculated following the standard methods of crystal optics; for $\theta=0$, it is [11]

$$\alpha_z=\frac{n_o\alpha_e-n_o/n_e(\alpha_e/n_e-\alpha_o/n_o)\sin^2\beta}{\sqrt{n_o^2-\sin^2\beta}}. \tag{A8}$$

[1] A. Saupe, Mol. Cryst. Liq. Cryst. **21**, 211 (1973).
[2] P. E. Cladis, W. van Saarloos, P. L. Finn, and A. R. Kortan, Phys. Rev. Lett. **58**, 222 (1987).
[3] S. Thiberge, C. Chevallard, J. M. Gilli, and A. Buka, Liq. Cryst. **26**, 1225 (1999).
[4] L. Leger-Quercy, Ph.D. Thesis, Université Paris-Sud, 1976 (unpublished); J. M. Gilli, S. Thiberge, A. Vierheilig, and F. Fried, Liq. Cryst. **23**, 619 (1997).
[5] F. Simoni, J. Phys.: Condens. Matter **11**, 439 (1999).
[6] L. Csillag, N. Éber, I. Jánossy, N. Kroó, V.F. Kitaeva, and N. N. Sobolev, Mol. Cryst. Liq. Cryst. **89**, 287 (1982).
[7] H. L. Ong, Appl. Phys. Lett. **46**, 822 (1985).
[8] J. J. Wu, G. S. Ong, and S. H. Chen, Appl. Phys. Lett. **53**, 1999 (1988).
[9] B. Ya. Zeldovich, N. V. Tabiryan, and Yu. S. Chilingaryan, Zh. Eksp. Teor. Fiz. **81**, 72 (1981) [Sov. Phys. JETP **54**, 32 (1981)].
[10] I. Jánossy, J. Nonlinear Opt. Phys. Mater. **8**, 361 (1999).
[11] L. Marrucci, D. Paparo, P. Maddalena, E. Massera, E. Prudnikova, and E. Santamato, J. Chem. Phys. **107**, 9783 (1997).
[12] N.V. Tabiryan, Opt. Spektrosk. **58**, 1142 (1985) [Opt. Spectrosc. **58**, 697 (1985)].
[13] I. Jánossy and A. D. Lloyd, Mol. Cryst. Liq. Cryst. **203**, 77 (1991).
[14] E. Benkler (private communication).
[15] S. K. Srivatsa and G. S. Ranganath, Phys. Rev. E **60**, 5639 (1999).
[16] X. Zhuang, L. Marrucci, and Y. R. Shen, Phys. Rev. Lett. **73**, 1513 (1994).